

## Relaxation times of nanoscale deformations on the surface of a polymer thin film near and below the glass transition

R. M. Papaléo, R. Leal, W. H. Carreira, and L. G. Barbosa

Faculty of Physics, Catholic University of Rio Grande do Sul, Av. Ipiranga 6681, Caixa Postal 1429, 90619-900 Porto Alegre, Brazil

I. Bello\* and A. Bulla

Institute of Physics, Federal University of Rio Grande do Sul, Av. Bento Gonçalves 9500, Porto Alegre, Brazil

(Received 2 May 2006; revised manuscript received 10 July 2006; published 28 September 2006)

We report on measurements of relaxation times of nanometer-sized deformations resulting from the impact of individual energetic ions on poly(methyl methacrylate) surfaces at temperatures close to and below the glass transition  $T_g$ . The temporal evolution of the dimensions of the deformations is well described by a stretched exponential function, but with relaxation times  $\tau(T)$  many orders of magnitude smaller than bulk values at the same  $T$ . The local  $T_g$  was around 86 °C, roughly 30 °C below the conventional bulk  $T_g$ . At the vicinity of the local  $T_g$ ,  $\tau(T)$  follows the Vogel-Fulcher type of  $T$  dependence, but at lower  $T$  a transition towards a less steep behavior is seen.

DOI: 10.1103/PhysRevB.74.094203

PACS number(s): 68.47.Mn, 61.80.Jh, 61.82.Pv, 62.20.Fe

The deformation and flow of *macroscopic* volumes of amorphous polymers have been extensively studied for many decades, resulting in a detailed description of the viscoelastic response of such materials.<sup>1</sup> The theoretical understanding of the viscous slowdown and the relaxation behavior of glasses, either polymeric or nonpolymeric, is, however, far from being complete and is still a major challenge for theorists.<sup>2,3</sup> This is particularly true for polymers in thin film and other constrained geometries, which may have physical properties different from those of the bulk, because of the presence of interfaces<sup>4-7</sup> and molecular confinement effects.<sup>8,9</sup> In advanced polymer-based materials, conditions of constraint in one or more dimensions are often present, e.g., in copolymers, nanocomposites, or porous membranes. Recently, new technologies or processes have been proposed, which are based on the local heating and deformation of tiny volumes of polymers (such as thermoelectrical nanolithography<sup>10</sup> or thermomechanical data storage<sup>11</sup>). The control and development of such processes and the evaluation of the stability of the devices constructed in confined geometries demands a solid knowledge of the relaxation behavior of *nanoscopic* volumes of polymers. In this paper, we report on the relaxation behavior of *nanometer-sized* deformations structured on polymer surfaces by the impact of individual energetic ions.

A heavy ion penetrating a solid at sufficiently high velocity deposits a large amount of energy at a fast rate in a small ( $\sim 1$  nm) region around its path.<sup>12</sup> Because of that, melting,<sup>13</sup> bond breaking, and particle ejection<sup>14</sup> may occur in the *core* of the impact, forming a crater. In addition, due to the large energy gradient built up in the core region, a pressure pulse may also be produced,<sup>15</sup> transferring, coherently, momentum for atoms and molecules sitting far from the ion track core. This process may be gentle enough to desorb intact thermally labile proteins<sup>16</sup> or to displace chunks of materials (in some cases with preserved crystal lattice<sup>17</sup>), which appear as tiny raised regions on the surface, few nm high and tens of nanometers long.<sup>18,19</sup> An impact feature (also called a surface track) induced by a 20 MeV Au ion on a glassy poly(methyl

methacrylate) (PMMA) film can be seen in Fig. 1. It may be divided into three regions: the crater [ $C$  in Fig. 1(f)], the tail [an elongated protrusion behind the crater;  $T$  in Fig. 1(f)], and the rims [hillocks showing up along the *sides* of the crater walls;  $R$  in Fig. 1(f)]. If the target temperature during the bombardment is higher than a critical temperature  $T_R$ , the tails relax and disappear completely.<sup>20</sup> We have recently shown that  $T_R$  can be used as a measure of the glass transition temperature,  $T_g$ .<sup>20</sup> Here, the relaxation dynamics of such nanodeformations has been followed in greater detail by carefully measuring their sizes as a function of time at various temperatures. Characteristic relaxation times were obtained for the volume, length, and height of the nanostructures. A large decrease of the average local relaxation times, in comparison to values of bulk PMMA, was observed with a corresponding decrease in the local  $T_g$ . The temperature dependence of  $\tau$  follows the classical Vogel-Fulcher relation for  $T$  in the vicinity of  $T_g$ , but at the lowest temperatures tested it was found a transition to a less steep dependence, apparently of an Arrhenius type.

Thin films (80–100 nm thick) of poly(methyl methacrylate) were spun onto Si substrates from solutions of nearly monodisperse powders in toluene ( $M_w = 3.6 \times 10^5$  u and  $8.65 \times 10^5$  u,  $M_w/M_n < 1.15$ , Polymer Standards Service) and subsequently annealed at 130 °C for 2 h. The samples were bombarded by a scanned beam of 20 MeV Au ions from a 3 MV Tandem ion implanter in vacuum. A hollow Cu sample holder with a heating stage and a cooling system (cooling rate  $\approx 20$  °C/s; for details of the experimental setup, see Ref. 20) was used for the bombardments and *in situ* relaxation of the films. Samples were irradiated at grazing angles of incidence ( $6^\circ$  with respect to the surface) at ten different temperatures  $T = 55, 60, 65, 75, 85, 89, 91, 94, 96$ , and 98 °C. The exposure to the beam lasts roughly 0.5 s and is accomplished by moving back and forth a shutter located in front of the targets, resulting in an impact density of roughly 4 ions/ $\mu\text{m}^2$ . The targets were held at the irradiation temperature for a predetermined time and immediately quenched to room temperature in order to “freeze” the mor-

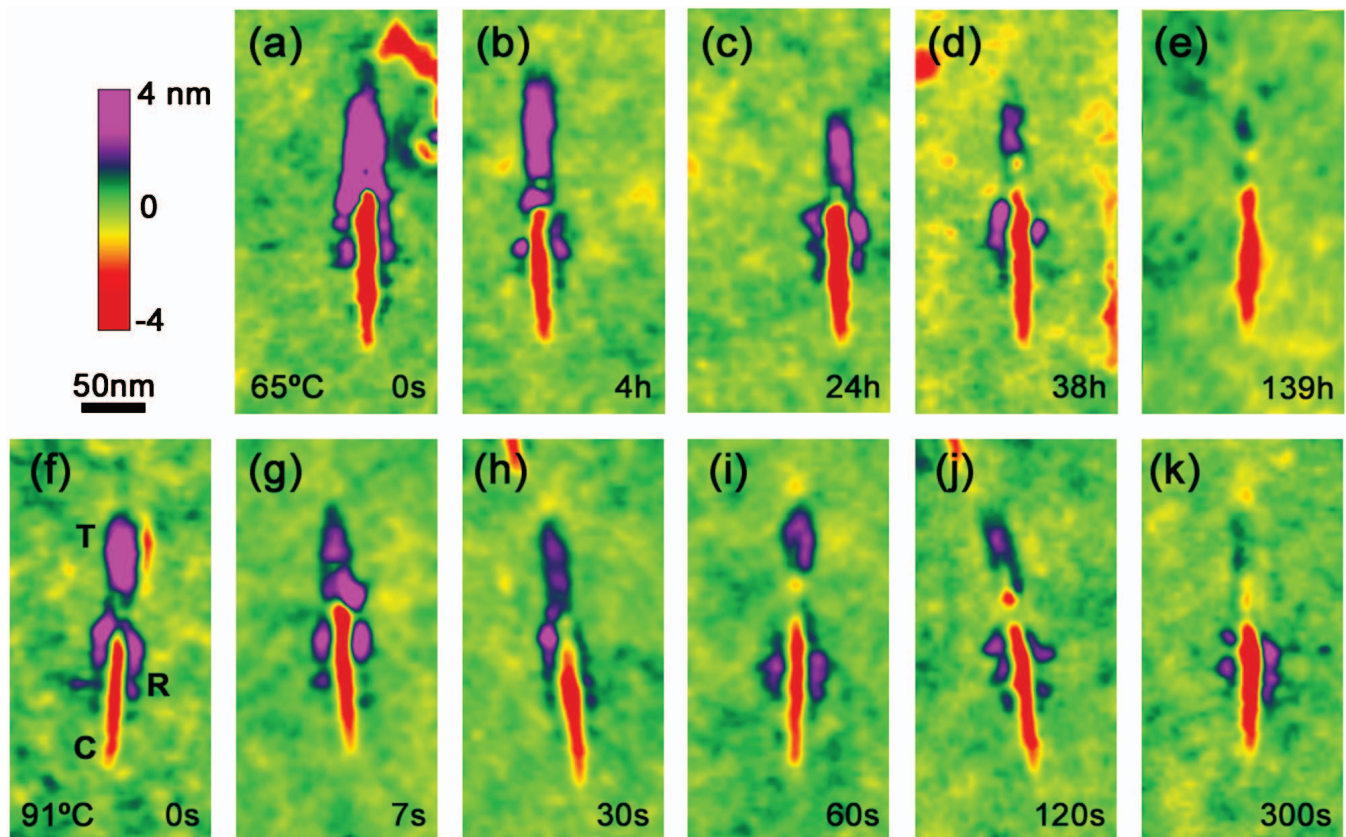


FIG. 1. (Color) Sequence of SFM images showing the typical stages of the relaxation dynamics of the impact features at 65 °C (a)–(e) and at 91 °C (f)–(k). The elapsed time  $t$  between the bombardment and the cooling are given in the figure for each image. In the frame (f), the crater, the tail, and the rim are identified by the letters C, T, and R, respectively.

phology of the relaxed deformations (as  $T_{amb} \ll T_g$ ) for subsequent imaging with scanning force microscopy (SFM). A series of samples was irradiated at each temperature  $T$ , covering a suitable range of annealing times (from few seconds to a couple of weeks) in order to map the various stages of the relaxation process. The cooling of the samples down to a slow-relaxing condition plus the bombardment time take at most  $\sim 2$  s; thus, in our present setup we are limited to assess relaxation in a time scale not faster than a second or so. The morphology and dimensions of the surface tracks were determined *ex situ* in a Nanoscope IIIa SFM (Digital Instruments) in the Tapping Mode, using NanoProbe Si tips. In order to minimize tip-surface interactions when probing a sample, the damping of the free oscillation of the cantilever was kept to a minimum value compatible with a stable imaging of the surface. The scanning frequency was always 1 or 2 Hz and the axis of fast scanning was perpendicular to the direction of ion incidence. Quantitative analysis of the SFM data was performed only on images captured with high-quality tips in order to minimize systematic errors due to tip shape. A detailed study on the influence of the tip on the metrology of surface tracks has been published elsewhere.<sup>19,21</sup>

Figure 1 shows a series of SFM images which give representative snapshots of impact features allowed to relax (at 65 °C and 91 °C) for different times before quenching to room temperature. The images depict the qualitative changes

observed in the morphology of the protrusions and craters as a function of time for the various temperatures tested. It is seen in Fig. 1 that the size of the tails decreases continuously. For 91 °C, they are fully relaxed  $\sim 300$  s after the ion impact [Figs. 1(f)–1(k)]. In contrast, the rims surrounding the central region of the craters, and the craters themselves, are much more stable than the tails. This means the relaxation process is not simply regulated by an effective relaxation time of the film, otherwise all structures would relax at a similar rate. Local variations in  $\tau$  are clearly present. The rims (and also the craters) are presumably chemically modified due to the radiation-induced bond reconstruction processes occurring at the *core* of the impact region.<sup>14</sup> The high thermal stability of the crater walls, evident in Fig. 1, suggests this is a highly cross-linked region. A full discussion on the behavior of the rims and craters will be presented elsewhere. Here we focus on the relaxation dynamics of external areas of the impact features (the tails), outside the region of chemical damage. Phase imaging performed on such areas reveals surfaces with similar properties as the unbombarded area.<sup>20,21</sup> The tails are here taken as a volume of pristine PMMA molecules, but with a built-in stress beyond yield.

The features depicted in Fig. 1 are representative of the *average* dimensions of the deformation for each relaxing time. There is, however, a significant statistical fluctuation of the *initial*, i.e., unrelaxed, volumes of the deformations over the bombarded area (Fig. 2). This seems to originate mainly

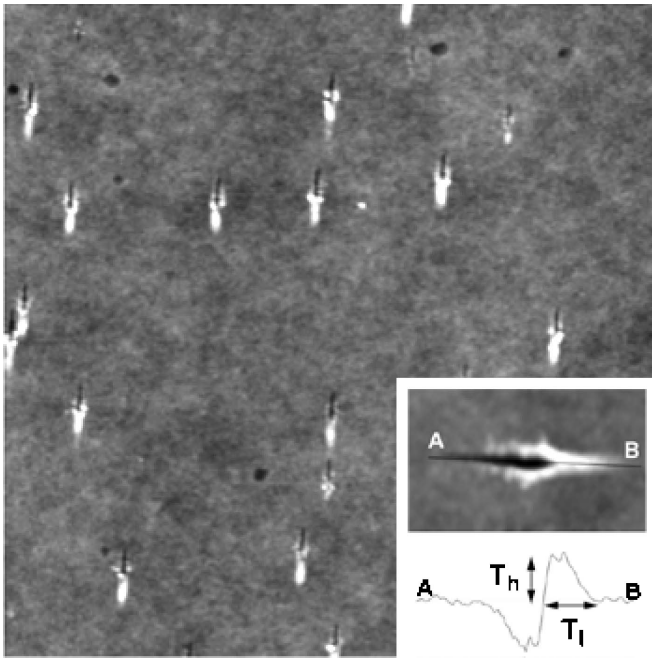


FIG. 2. SFM image of a PMMA film bombarded by 20 MeV Au ions at room temperature. The standard deviation of hillock volumes is around 30%. Smaller defects, attributed to a lower energy beam not filtered out by the beam switch magnet, are also seen. The grayscale covers height variations in the 10 nm range. The inset shows a line profile  $AB$  along a particular impact feature and defines the tail length ( $T_l$ ) and height ( $T_h$ ).

from fluctuations in the *local* linear energy transfer  $dE/dx$  at the surface (which controls the size of the ion-induced deformations<sup>22</sup>). Such size dispersion propagates to the relaxed targets and give rises to relatively large error bars on the average dimensions. The trend for the mean values, however, is clear and systematic, as discussed below.

The average length  $l$  and volume  $V$  of the tails are plotted as a function of time and temperature in Fig. 3. All dimensions (including the maximum height, not shown) could be fitted to the Kohlrausch-Williams-Watts (KWW) relaxation function,

$$X(t) = X_0 \exp(-t/\tau)^\beta, \quad (1)$$

where  $t$  is the time,  $\tau$  is the effective relaxation time,  $X$  is the particular dimension being considered, and  $0 < \beta < 1$ . The nonexponential behavior of the structural relaxation is a characteristic of polymer glasses and is formally equivalent to the existence of a distribution of relaxation times, with a width monotonously decreasing with  $\beta$ . For PMMA, the reported values of  $\beta$  are around 0.4. As the size fluctuations are large and the number of points on the relaxation curves is limited for an unambiguous evaluation of the stretching parameter  $\beta$ , a fixed  $\beta=0.4$  was used in Eq. (1), except for  $T < 75^\circ\text{C}$  where  $\beta$  approaching unity gave clearly better fits.

In Fig. 3, the time  $t=1$  s (and not  $t=0$  s) corresponds to immediate cooling after the bombardment. This was done to

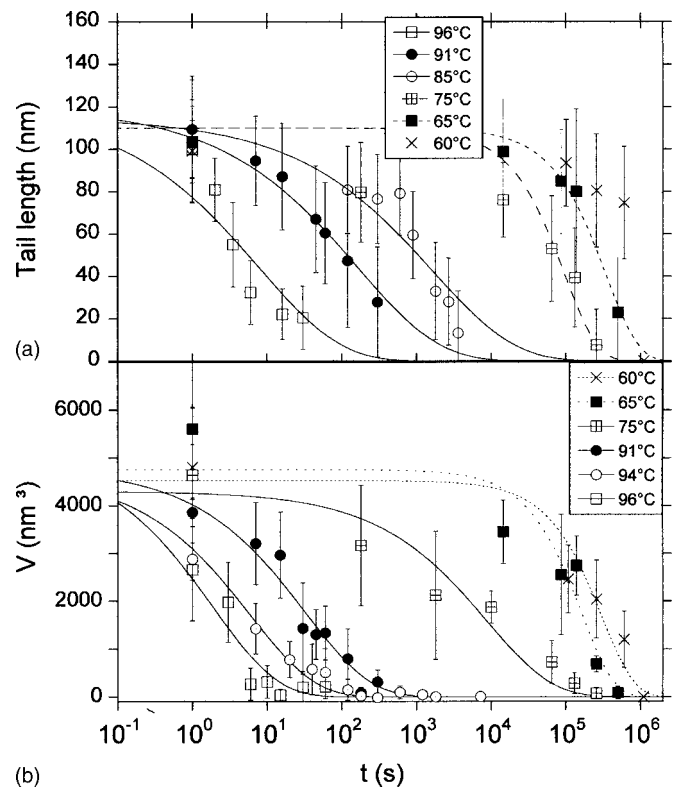


FIG. 3. Average size of protrusions induced by 20 MeV Au ions impacting PMMA thin films as a function of time and temperature: (a) tail length and (b) tail volume. The solid lines are stretched exponential fits with  $\beta=0.4$  and broken lines are simple exponential fits ( $\beta=1$ ).

better represent the finite cooling time. For  $T < 85^\circ\text{C}$ , the cooling time is negligible compared to the relaxation time and the measurement at  $t \sim 1$  s is a very good approximation to the “true” initial dimension. This is not the case for temperatures above  $91^\circ\text{C}$ . For fitting purposes, the initial dimensions at the highest temperatures were forced not to deviate (within error bars) from the average  $X_0$  at the lowest temperatures (i.e.,  $V_0 \sim 4500 \text{ nm}^3$ ,  $l_0 \sim 110 \text{ nm}$ , and  $h_0 \sim 4 \text{ nm}$ ).

The relaxation times of the tail length ( $\tau_l$ ), the maximum height ( $\tau_h$ ), and volume ( $\tau_v$ ), obtained from Eq. (1) for each temperature, are depicted in Fig. 4, covering the interval of  $10^0$  s to  $10^6$  s. The linear  $\tau$  ( $\tau_l$  and  $\tau_h$ ) are always smaller than  $\tau_v$ , as expected (for an isotropic exponential relaxation  $\tau_v = 1/3 \tau_{\text{linear}}$ ). The measured relaxation times were much smaller than those typical of bulk PMMA of comparable  $M_w$ . Accordingly, the local glass transition  $T_g^{\text{local}}$ , defined as  $\tau(T_g) = 100$  s, was around  $86^\circ\text{C}$ , roughly  $30^\circ\text{C}$  below the bulk  $T_g$ .<sup>23</sup> The portion of the data lying at temperatures near and above  $T_g^{\text{local}}$  was adjusted to the Vogel-Fulcher-Tammann (VFT) equation (solid and dashed lines in Fig. 4),

$$\tau(T) = \tau_\infty \exp\left(\frac{B}{T - T_0}\right). \quad (2)$$

The best fit for the volume of the deformations was obtained with  $B_{\text{def}} = 2073 \pm 256 \text{ K}$  and  $T_0 = 293 \pm 7 \text{ K}$ , using a fixed

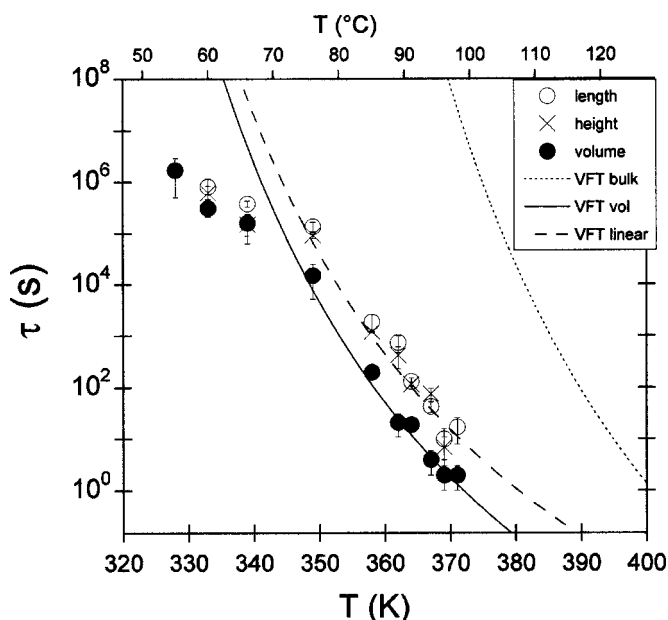


FIG. 4. Temperature dependence of the characteristic relaxation times for the volume, length, and height of the nanodeformations. The solid and dashed lines depict the Vogel-Fulcher equation [Eq. (2)] adjusted to the high temperature portion of the experimental data. For comparison, a VFT curve required to give a  $T_g$  of 389 K (typical of bulk PMMA) is also displayed as a dotted line. The glass transition temperature is defined as  $\tau(T_g)=100$  s. At 55 °C, full relaxation of the deformations could not be achieved, but a  $\tau$  was still extracted.

$\tau_\infty=10^{-12}$  s. For comparison, a VFT curve simulated with a standard bulk PMMA  $T_o$  of 323 K and  $T_g^{bulk}=389$  K (Ref. 23) was also added in Fig. 4. For this fit,  $B_{bulk}$  ( $=2150$  K) was adjusted to give  $\tau(T_g^{bulk})=100$  s, using the same high-temperature prefactor  $\tau_\infty=10^{-12}$  s. Thus the shifts in the VFT curves of the nanodeformations and typical bulk PMMA can be roughly parameterized by a shift in  $T_o$ ,  $\Delta T_o$  similar to  $\Delta T_g=T_g^{bulk}-T_g^{local}\sim 30$  °C. The effective activation temperature  $B_{def}$  is similar to the bulk value and to other estimations from PMMA thin films.<sup>24</sup> At low temperatures, a deviation from the VFT type of behavior is seen. The temperature dependence of  $\tau$  becomes less steep for  $\tau$  larger than  $\sim 10^5$  s, tending to what appears to be an Arrhenius-type dependence.

Structural relaxation in polymer thin films may be perturbed, as compared to the bulk, by essentially three factors: the close proximity of the free surface and substrate interfaces and finite size or confinement effects.<sup>25</sup> Several polymeric systems exhibited  $T_g$  reductions<sup>4-6,26</sup> when only the surface region was probed or when free surfaces dominate the film behavior. For PMMA thin films deposited on Si substrates, a decrease of 5–6 °C in  $T_g$  was observed at the free-surface region,<sup>4</sup> whereas at the interface region hydrogen bonds between the polar groups of the PMMA side chain and the native  $\text{SiO}_x$  layer lead to an increase in  $T_g$  of up to 12 °C.<sup>4,6</sup> The fast relaxation rates seen in our experiments are a clear indication of an enhanced surface mobility in PMMA. However, the local  $T_g$  depression at the deforma-

tions ( $\sim 30$  °C) is even larger than those of PMMA free surfaces, implying the (local) rates of relaxation at the deformations are much faster than those of the average PMMA surface. Considering that the protrusions are formed after the sudden expansion of the material in the core of the impact, at strain rates of the order of  $10^9$ /s,<sup>22</sup> the fast relaxation of the deformations may be related to a decreased density<sup>27</sup> at these regions, possibly combined with the high internal stress, that reportedly speed up the dynamics.<sup>28</sup> Even though those are sensible arguments, we lack means of probing the exact tail structure and thus to test quantitatively such hypotheses.

The transition from a VFT towards an Arrhenius-like temperature dependence of  $\tau$  as the glass transition is approached (in our case at  $T < T_g^{local} - 10$  °C) has been observed in bulk polymeric glasses,<sup>29</sup> as the material departs from an equilibrium situation. Different theoretical scenarios may account for such a transition.<sup>30-32</sup> In the Adam and Gibbs model of relaxation of glass formers,<sup>31</sup>  $\tau(T)=\tau_\infty \exp(C/TS_c)$ , where  $C$  is a constant and  $S_c(T)$  is the configurational entropy. For  $T_g < T < T_B$  (with  $T_B$  around  $T_g+100$  °C for polymers), where the VFT relation Eq. (1) applies,  $S_c(T)$  can be taken<sup>33</sup> as  $S_c(T)=S_\infty(1-T_o/T)$ . For  $T < T_g$ , the temperature dependence of  $S_c$ , measured for different glass formers, is weak<sup>33</sup> and, accordingly,  $\tau(T)$  would increase less steeply with decreasing  $T$ . If  $S_c$  is approximately constant, an Arrhenius type of dependence would be obtained. Such a crossover in the relaxation process can also be interpreted in terms of the appearance of finite size or confinement effects. The dramatic slowing down of structural relaxation of amorphous polymers upon cooling is often attributed to the necessity of cooperative rearrangements<sup>4,25,31</sup> inside regions of the sample with sizes  $z^*(T)$  ( $\propto S_c^{-1}$ ) that increase with decreasing temperature. This means the effective activation energy of the process is temperature dependent through  $z^*(T)$ . When the length of cooperativity comprises the whole object, the effective activation energy becomes independent of temperature and an Arrhenius behavior is expected for the relaxation times upon further cooling. Such scenario suggests the volume of the cooperating regions at  $T \sim 75$  °C would be comparable to that of the whole deformation (of the order of  $10^3$  nm<sup>3</sup>). This volume is large if compared to estimations of  $z^*(T_g)$  of few nm by Hempel *et al.*<sup>34</sup> or Forrest *et al.*,<sup>35</sup> but other estimations for polymers vary from 4–15 nm.<sup>32</sup> Thus, a volume of  $\sim 10^3$  nm<sup>3</sup>, at  $T$  below  $T_g$  is still reasonable. Experiments are being performed to follow the relaxation behavior of deformations produced at nongrazing impact angles, that are shorter by a factor of 3. The crossover temperature would be higher for smaller deformations, if it is coupled to finite size effects.

In summary, the relaxation dynamics of nanodeformations structured on PMMA surfaces by the impact of *individual* ions has been followed at temperatures near and below the glass transition. The temporal evolution of the average dimensions of the deformations could be described by standard relaxation functions, but with relaxation times  $\tau(T)$  roughly four orders of magnitude smaller than typical bulk values at the same  $T$ . Accordingly, a local glass transition has been

assigned that lies roughly 30 °C below the conventional  $T_g$  of the polymer and approximately 25 °C below the surface  $T_g$ .<sup>4</sup> The temperature dependence of the relaxation times shows a smooth transition from a VFT shape towards a weaker (Arrhenius-like) dependence below  $T_g$ , as observed for several polymers in the bulk. While the Arrhenius behavior for  $\tau(T)$  in the nonequilibrium glassy state is predicted by different models because the length scales of cooperative motion become temperature independent (or

weakly dependent), such crossover may also be related to the appearance of finite size effects at low  $T$  due to the limited dimensions of the deformations. Further experiments are being conducted to vary the size of the deformations and test the last hypothesis.

The authors would like to acknowledge the Brazilian agencies CAPES, CNPq, and FAPERGS for financial support.

\*Deceased.

- <sup>1</sup>J. D. Ferry, *Viscoelastic Properties of Polymers* (John Wiley & Sons, New York, 1970).
- <sup>2</sup>C. A. Angell, K. L. Ngai, G. B. McKenna, and P. F. McMillan, *J. Appl. Phys.* **88**, 3113 (2000).
- <sup>3</sup>D. Kivelson, G. Tarjus, X. Zhao, and S. A. Kivelson, *Phys. Rev. E* **53**, 751 (1996).
- <sup>4</sup>R. D. Priestley, C. J. Ellison, L. J. Broadbelt, and J. M. Torkelson, *Science* **309**, 456 (2005).
- <sup>5</sup>J. A. Forrest, C. Svanberg, K. Révész, M. Rodahl, L. M. Torrel, and B. Kasemo, *Phys. Rev. E* **58**, R1226 (1998).
- <sup>6</sup>J. L. Keddie, R. A. L. Jones, and R. A. Cory, *Faraday Discuss.* **98**, 219 (1994); H. Richardson, I. Lopez-Garcia, M. Sferrazza, and J. L. Keddie, *Phys. Rev. E* **70**, 051805 (2004).
- <sup>7</sup>J. H. Teichroeb and J. A. Forrest, *Phys. Rev. Lett.* **91**, 016104 (2003); J. S. Sharp and J. A. Forrest, *ibid.* **91**, 235701 (2003).
- <sup>8</sup>B. Jérôme and J. Commandeur, *Nature (London)* **386**, 589 (1997).
- <sup>9</sup>S. H. Anastasiadis, K. Karatasos, G. Vlachos, E. Manias, and E. P. Giannelis, *Phys. Rev. Lett.* **84**, 915 (2000).
- <sup>10</sup>S. F. Lyuksyutov, R. A. Vaia, P. B. Paramonov, S. Juhl, L. Waterhouse, R. M. Ralich, G. Sigalov, and E. Sancaktar, *Nat. Mater.* **2**, 468 (2003).
- <sup>11</sup>P. Vettinger, M. Despont, U. Düring, M. A. Lantz, H. E. Rothuizen, and G. K. Binnig, in *Nanoelectronics and Information Technology*, edited by R. Waser (Wiley-VCH, Weinheim, 2003).
- <sup>12</sup>R. L. Fleischer, P. Price, and R. M. Walker, *Nuclear Tracks in Solids* (University of California Press, Berkeley, 1975).
- <sup>13</sup>M. Toulemonde, Ch. Dufour, A. Meftah, and E. Paumier, *Nucl. Instrum. Methods Phys. Res. B* **166&167**, 903 (2000).
- <sup>14</sup>R. M. Papaléo, P. Demirev, J. Eriksson, P. Hakansson, B. U. R. Sundqvist, and R. E. Johnson, *Phys. Rev. Lett.* **77**, 667 (1996).
- <sup>15</sup>R. E. Johnson, B. U. R. Sundqvist, A. Hedin, and D. Fenyő, *Phys. Rev. B* **40**, 49 (1989).
- <sup>16</sup>R. E. Johnson and B. U. R. Sundqvist, *Phys. Today* **45**, No. 3, 28 (1992).
- <sup>17</sup>D. D. N. B. Daya, A. Hallén, P. Hakansson, B. U. R. Sundqvist, and C. T. Reimann, *Nucl. Instrum. Methods Phys. Res. B* **103**, 454 (1995).
- <sup>18</sup>R. Neumann, *Nucl. Instrum. Methods Phys. Res. B* **151**, 42 (1999).
- <sup>19</sup>R. M. Papaléo, in *Fundamentals of Ion-Irradiated Polymers*, edited by D. Fink (Springer, Berlin, 2004), pp. 207–250.
- <sup>20</sup>R. M. Papaléo, L. D. de Oliveira, L. S. Farenzena, M. A. de Araújo, and R. Livi, *Phys. Rev. B* **62**, 11273 (2000).
- <sup>21</sup>L. S. Farenzena, R. P. Livi, M. A. de Araújo, G. Garcia Bermudez, and R. M. Papaléo, *Phys. Rev. B* **63**, 104108 (2001).
- <sup>22</sup>E. Bringa, R. E. Johnson, and R. M. Papaléo, *Phys. Rev. B* **65**, 094113 (2002).
- <sup>23</sup>K. Fuchs, C. Friedrich, and J. Weese, *Macromolecules* **29**, 5893 (1996).
- <sup>24</sup>J. S. Sharp and J. A. Forrest, *Eur. Phys. J. E* **1**, 23 (2003).
- <sup>25</sup>J. A. Forrest and R. A. L. Jones, in *Polymer Surfaces, Interfaces, and Thin Films*, edited by A. Karim and S. Kumar (World Scientific, Singapore, 2000), p. 251.
- <sup>26</sup>K. Fukao, S. Uno, Y. Miyamoto, A. Hoshino, and H. Miyaji, *Phys. Rev. E* **64**, 051807 (2001).
- <sup>27</sup>According to free volume arguments, a change in density of only ~1% suffices to change the  $T_g$  value by 40 K (Ref. 24). Thus, in our case, a change in density of ~0.7% would be required in the tails, if stress effects are not considered.
- <sup>28</sup>F. M. Capaldi, M. C. Boyce, and G. C. Rutledge, *Phys. Rev. Lett.* **89**, 175505 (2002).
- <sup>29</sup>P. A. O'Connell and G. B. McKenna, *J. Chem. Phys.* **110**, 11054 (1999).
- <sup>30</sup>E. A. Di Marzio, *J. Res. Natl. Inst. Stand. Technol.* **102**, 135 (1997).
- <sup>31</sup>G. Adam and J. H. Gibbs, *J. Chem. Phys.* **43**, 139 (1965).
- <sup>32</sup>B. M. Erwin and R. H. Colby, *J. Non-Cryst. Solids* **307-310**, 225 (2002).
- <sup>33</sup>R. Richert and C. A. Angell, *J. Chem. Phys.* **108**, 9016 (1998).
- <sup>34</sup>E. Hempel, G. Hempel, A. Hensel, C. Schick, and E. Donth, *J. Phys. Chem. B* **104**, 2460 (2000).
- <sup>35</sup>J. A. Forrest and K. Dalnoki-Veress, *Adv. Colloid Interface Sci.* **94**, 167 (2001).